Modeling uncertainty in three-dimensional heat transfer problems

Xiaoliang Wan[†], Dongbin Xiu and George Em Karniadakis[†]

Abstract

We present a generalized polynomial chaos method to solve the steady and unsteady heat transfer problems with uncertainty in boundary conditions, diffusivity coefficient and forcing terms. The stochastic inputs and outputs are represented spectrally by employing the orthogonal polynomial functionals from the Askey scheme, as a generalization of the original polynomial chaos idea of Wiener [1]. A Galerkin projection in random space is applied to derive the equations in weak form, and a parallel spectral/hp element method is employed to solve the resulting set of deterministic equations. Simulations in three-dimensional domains with stochastic dimension 38 and about 150 million unknowns are presented here for the first time.

Contents

[†]Division of Applied Mathematics, Brown University, Providence, RI 02912
(xlwan@dam.brown.edu, gk@dam.brown.edu)

1 Introduction

Traditionally, heat transfer analysis is based on deterministic mathematical models, where the physical properties and boundary conditions are specified precisely. In reality, such parameters can be uncertain due to the heterogeneity of the medium, inaccurate measurements or small scale variations. To deal with uncertainty, statistical and non-statistical computational strategies have been employed. The statistical approaches, e.g. Monte Carlo simulations, can be prohibitively time-consuming, especially for three-dimensional complex systems. Non-statistical approaches approximate the stochastic equations in an analytical manner. Such methods include perturbation methods [2, 3, 4, 5], Neumann expansions [6, 7, 8], a weighted integral method [9, 10], etc. A common drawback of these methods is that they are restricted to small random inputs and outputs.

Another non-statistical approach, called *polynomial chaos*, is based on the homogeneous chaos theory of Wiener [1]. It models the uncertainty by a spectral expansion based on Hermite orthogonal polynomials in terms of Gaussian random variables. This method was applied by Ghanem and co-workers to various problems in mechanics [11, 12, 13, 14]. A broader framework, called the "generalized polynomial chaos", was introduced in [15, 16, 17]. This method employs a broad family orthogonal polynomials as the expansion basis to represent non-Gaussian processes more efficiently; it includes the classical Hermite polynomial chaos as a subset. More recently, work by Babuska and co-workers further examined the mathematical properties of these expansions [18, 19, 20].

In this work, we focus on the three-dimensional steady and unsteady heat transfer problems with random heat conductivity. In particular, we assume that the random input has *short correlation length*, which results in high-dimensional polynomial chaos expansion. The semi-discrete systems consists of 780 deterministic three-dimensional heat conduction equations, and thus it is solved on parallel computers.

2 Generalized polynomial chaos

The generalized polynomial chaos is based on the orthogonal polynomial expansions of random variables. A general second-order random process $X(\omega)$ can be expressed as

$$X(\omega) = \sum_{j=0}^{\infty} a_j \Phi_j(\boldsymbol{\xi}(\omega)), \tag{2.1}$$

where ω is the random event, $\Phi_j(\boldsymbol{\xi})$ the generalized polynomial chaos of order p in terms of multi-dimensional random variables $\boldsymbol{\xi} = (\xi_1, \ldots, \xi_n)$, and $\{a_j\}$ the expansion coefficients. The orthogonal basis $\{\Phi_j\}$ satisfies

$$\langle \Phi_i, \Phi_j \rangle = \langle \Phi_i^2 \rangle \delta_{ij}, \tag{2.2}$$

where δ_{ij} is the Kronecker delta, and $\langle f, g \rangle = \mathbb{E}[fg]$ is the ensemble average. Here the ensemble average is defined as the inner product in the Hilbert space

in terms of the random vector $\boldsymbol{\xi}$

$$\langle f(\boldsymbol{\xi}), g(\boldsymbol{\xi})\rangle = \int f(\boldsymbol{\xi})g(\boldsymbol{\xi})w(\boldsymbol{\xi})\mathrm{d}\boldsymbol{\xi}, \tag{2.3}$$

or

$$\langle f(\boldsymbol{\xi}), g(\boldsymbol{\xi})\rangle = \sum_{\boldsymbol{\xi}} f(\boldsymbol{\xi})g(\boldsymbol{\xi})w(\boldsymbol{\xi}), \tag{2.4}$$

in the discrete case, where $w(\boldsymbol{\xi})$ denotes the weight function. For a certain random vector $\boldsymbol{\xi}$, the generalized polynomial chaos $\{\Phi_j\}$ can be chosen in such a way that its weight function has the same form as the probability distribution function of $\boldsymbol{\xi}(\omega)$.

3 The Karhunen-Loeve decomposition

Let $h(\mathbf{x};\omega)$ denotes the random process and $R_{hh}(\mathbf{x},\mathbf{y})$ the correlation function. The Karhunen-Loeve(KL) decomposition [21] can be expressed as:

$$h(\mathbf{x};\omega) = \overline{h}(\mathbf{x}) + \sum_{i=0}^{\infty} \sqrt{\lambda_i}\phi_i(\mathbf{x})\xi_i(\omega), \tag{3.1}$$

where $\overline{h}(\mathbf{x})$ denotes the mean, and $\{\xi_i(\omega)\}$ is a set of uncorrelated random variables with zero mean and unit variance. Also, $\phi_i(\mathbf{x})$ and λ_i are the eigenfunctions and eigenvalues of the correlation function, respectively, i.e.,

$$\int_{\mathbf{D}} R_{hh}(\mathbf{x},\mathbf{y})\phi_i(\mathbf{y})\mathrm{d}\mathbf{y} = \lambda_i\phi_i(\mathbf{x}). \tag{3.2}$$

In practice, a truncated N-term decomposition of (3.1) is employed, where N is determined by the decay of the eigenvalues from (3.2) to ensure that the truncation error is acceptably small. Karhunen-Loeve decomposition thus provides a means of reducing dimensionality in random space.

4 Governing equation and numerical procedure

Let $\mathbf{D}$ be a bounded domain and denote by n the unit outward normal direction on $\partial\mathbf{D}$. Let $\mathbf{T} = [0,\infty)$ be the time domain, $\kappa = \kappa(\mathbf{x};\omega)$ the stochastic diffusivity, and $f = f(\mathbf{x},t;\omega)$ the stochastic source term. Let $\{\partial\mathbf{D}_d, \partial\mathbf{D}_n\}$ be a partition decomposition of $\partial\mathbf{D}$, where $\partial\mathbf{D}_d$ is the Dirichlet boundary and $\partial\mathbf{D}_n$ the Neumann boundary. The general form of the governing equation for the stochastic heat transfer problem can be expressed as

$$\alpha\frac{\partial u(\mathbf{x},t;\omega)}{\partial t} = \nabla\cdot[\kappa(\mathbf{x};\omega)\nabla u(\mathbf{x},t;\omega)] + f(\mathbf{x},t;\omega) \tag{4.1}$$

$$u(\mathbf{x},0;\omega) = u_0(\mathbf{x};\omega) \qquad \mathbf{x}\in\mathbf{D} \tag{4.2}$$

$$u(\mathbf{x},t;\omega) = u_d \qquad \mathbf{x}\in\partial\mathbf{D}_d \qquad \frac{\partial u(\mathbf{x},t;\omega)}{\partial n} = q \qquad \mathbf{x}\in\partial\mathbf{D}_n, \tag{4.3}$$

where $(\mathbf{x}, t; \omega) \in \mathbf{D} \times \mathbf{T} \times \Omega$, $\alpha = 0, 1$ in steady and unsteady case, respectively, the source term f and the diffusivity κ are prescribed data. Note here that if $\alpha = 0$, the initial condition is unnecessary.

By applying the generalized chaos expansion, we can expand the random process in eqn (4.1) in the following form:

$$u(\mathbf{x}, t; \omega) = \sum_{i=0}^{M} u_i(\mathbf{x}, t)\Phi_i(\boldsymbol{\xi}), \tag{4.4}$$

where $\boldsymbol{\xi} = (\xi_1, \ldots, \xi_n)$ with a dimensionality n determined by the random inputs. Similar expansion is applied to other random processes, e.g. κ, f, etc. The number $(M+1)$ is determined by the dimensionality of the chaos expansion (n) and the highest order (p) of the polynomials $\{\Phi_i\}$, where

$$(M + 1) = (n + p)!/(n!p!). \tag{4.5}$$

Introducing the chaos expansion into the governing equation (4.1), we obtain

$$\alpha \sum_{i=0}^{M} \frac{\partial u_i(\mathbf{x}, t)}{\partial t}\Phi_i = \sum_{i=0}^{M}\sum_{j=0}^{M} \nabla \cdot [\kappa_i(\mathbf{x})\nabla u_j(\mathbf{x}, t)]\Phi_i\Phi_j + \sum_{i=0}^{M} f_i(\mathbf{x}, t)\Phi_i. \tag{4.6}$$

Note M can be different for different processes, but for notational convenience we will keep the same M in all expansions. A Galerkin projection of the above equation onto $\{\Phi_k\}$ is then conducted. Multiplying eqn (4.6) by Φ_k, evaluating its expectation and taking into account the orthogonality of the basis, we get

$$\alpha \frac{\partial u_k(\mathbf{x}, t)}{\partial t} = \sum_{j=0}^{M} \nabla \cdot [b_{jk}(\mathbf{x})\nabla u_j(\mathbf{x}, t)] + f_k(\mathbf{x}, t) \qquad k = 0, \ldots, M \tag{4.7}$$

where $b_{jk}(\mathbf{x}) = \frac{1}{\langle\Phi_k^2\rangle} \sum_{i=0}^{M} \kappa_i(\mathbf{x})\langle\Phi_i\Phi_j\Phi_k\rangle$. Upon expanding initial/boundary conditions in a similar manner, we obtain a complete set of equations for each expansion coefficient.

4.1 Steady state equation

In this case, $\alpha = 0$. We employ a block Gauss-Seidel iteration method:

$$-\nabla \cdot (b_{kk}\nabla u_k^{n+1}) = \sum_{j=0, j\neq k}^{M} \nabla \cdot [b_{jk}\nabla u_j^n(\mathbf{x}, t)] + f_k(\mathbf{x}), \tag{4.8}$$

where the superscript n denotes the iteration step. The converge criterion is defined as

$$\frac{\|u_k^{n+1}(\mathbf{x}) - u_k^n(\mathbf{x})\|}{\sup \|u_k^1(\mathbf{x}) - u_k^0(\mathbf{x})\|} \leq \epsilon \qquad k = 0, 1, \ldots, M,$$

where $\epsilon > 0$ is the error control. In this paper, we use L_∞ norm and set $\epsilon = 10^{-9}$. The iterations normally converge within about 10 steps.

4

4.2 Unsteady equation

Here, $\alpha = 1$. We employ a mixed explicit-implicit approach and design a high-order temporal scheme in the following form,

$$\frac{\hat{u}_k(\mathbf{x}) - \sum_{q=0}^{J-1} \alpha_q u^{n-q}(\mathbf{x})}{\Delta t} = \sum_{q=0}^{J-1} \beta_q \Big[\sum_{j=0,j\neq k}^{M} \nabla \cdot \big(b_{jk}\nabla u_j(\mathbf{x})\big) \Big]^{n-q}, \quad (4.9)$$

$$\frac{\gamma_0 u_k^{n+1}(\mathbf{x}) - \hat{u}_k(\mathbf{x})}{\Delta t} = \nabla \cdot [b_{kk}\nabla u_k^{n+1}(\mathbf{x})] + f_k^{n+1}(\mathbf{x}), \quad (4.10)$$

where J is the order of accuracy in time and the superscript $(n+1)$ and $(n-q)$ denote the time level t^{n+1} and t^{n-q}, respectively. The values of the coefficients α_q, β_q and γ_0 in the scheme can be found in [22]. Spatial discretization can be obtained by any conventional method, e.g. finite difference, finite elements, etc. Here we employ the spectral/hp method to achieve high accuracy in space and flexible element control [22].

5 Numerical results

In this section, we consider the three-dimensional heat conduction in an electronic chip subject to random conductivity. Due to symmetry half of the computational domain is shown in Fig. 1. The boundary of the domain consists of four segments: the top Γ_T, the bottom Γ_B, the sides Γ_S and the boundaries of the cavity Γ_C. The correlation function for the stochastic input processes, e.g. κ, is assumed to have exponential form, i.e.

$$C(\mathbf{x}_1, \mathbf{x}_2) = e^{-|\mathbf{x}_1 - \mathbf{x}_2|/b} \quad (5.1)$$

where b is the correlation length. Since no analytical solution is available for the eigen-problem (3.2) in 3D, we developed a parallel numerical solver based on Nyström method and implicitly restarted Arnoldi method [23, 24]. In Fig. 2, we show the first 50 eigenvalues for $b = 1.0$. For the parallel spectral/hp element solver in space, 832 hexahedral elements are used in the domain. Within each element, sixth-order(Jacobi) polynomials are employed resulting in 190,825 degrees-of-freedom for one deterministic simulation. Second-order chaos and 38-term Karhunen-Loeve decomposition were employed, with the smallest eigenvalue being 4.4% of the largest one. This results in a 780-term expansion (see (4.5); for $n = 38, p = 2$); thus the total number of unknowns of the stochastic problem is 148,843,500. All simulations were run on 256 processors at the SGI 3800 (Department of Defense, ERDC).

5.1 Steady simulation: Hermite-chaos and Gaussian inputs

We now consider the 3D steady state heat conduction with random conductivity. Adiabatic boundary conditions are prescribed on Γ_S and Γ_B. The temperature
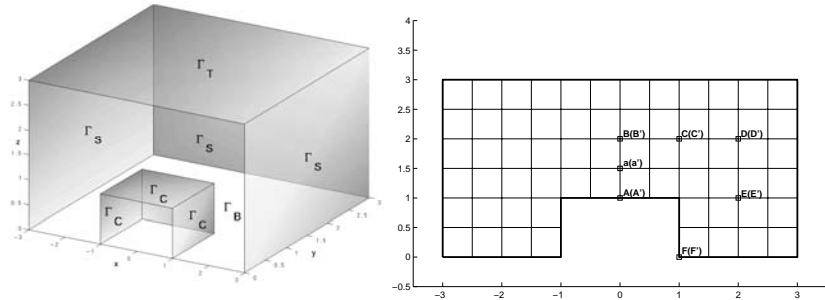
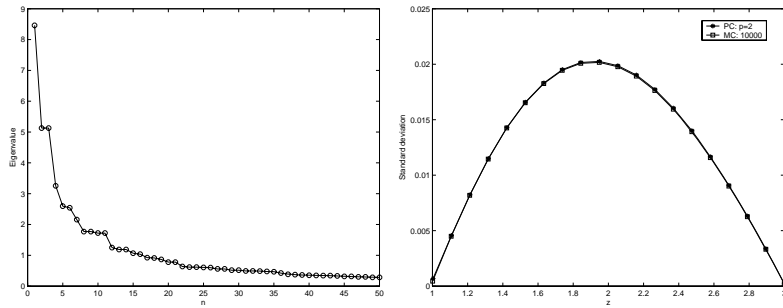Figure 1: Left: Half of the computational domain. Right: Reference points on planes y=0 and y=1.

Figure 2: Left: First 50 eigenvalues of exponential kernel with $b = 1$. Right: Standard deviation along the vertical centerline.

is set to be 0 on Γ_T and 1.0 on Γ_C. We assume that the source force is zero and the random field $\kappa(x; \omega)$ is a Gaussian process from the 38-term Karhunen-Loeve decomposition with $\sigma_\kappa = 0.2$. A second-order Hermite-chaos is employed for this case. The contours of the stochastic solution of the temperature field are plotted in Fig. 3. It is seen that the largest uncertainty, indicated by the standard deviation, occurs between the top and the cavity surface. Monte Carlo simulations are also conducted to verify the results from Hermite-chaos. To reach good agreement, 10,000 relizations are empoyed. In Fig. 2, the standard deviation along the vertical centerline is shown.
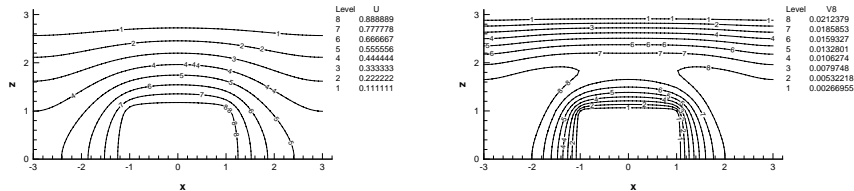

Figure 3: Contours on $y = 0$. Left: mean field. Right: standard deviation.

5.2 Unsteady simulation: Legendre-chaos and non-Gaussian inputs

Here we set flux boundary condition on Γ_C with $q|_{\Gamma_C} = 1$ and adiabatic boundary condition on Γ_B, Γ_S and Γ_T. Again, a zero source force is prescribed. We assume that $\kappa(x; \omega)$ is a random field resulted from the 38-term Karhunen-Loeve decomposition with the underlying random variables having uniform distribution, and $\sigma_\kappa = 0.2$. A second-order Legendre-chaos is employed for this case. Some reference points are shown in Fig. 1, where points without prime are located on $y = 0$ while their projection on $y = 1$ are the rest with prime. We are interested in the stochastic solution at these points and their cross-correlation coefficients. In Fig. 4, we show the evolution of the stochastic solution at reference points on $y = 0$, with mean on the left and COV(coefficient of variance) defined as $\text{COV}(\mathbf{x}, t) = \sigma_u(\mathbf{x}, t)/\mathbb{E}[u(\mathbf{x}, t; \omega)]$ on the right. It is seen that the mean temperature keeps growing over time while the COVs approach steady-state quickly. Relatively strong variation of COV is observed during the early transient period. In Fig. 5, the cross-correlation coefficients between reference points are plotted. It is observed that the statistics approach steady-state. Since the correlation length b of stochastic conductivity κ is 1.0, which is relatively small, we can observe that as the distance away from A increases, its influence to $B - F$ decreases up to about 20%. In Fig. 6, we show the evolution of *mean temperature* at some reference points on $y = 0$ with error bars indicating standard deviations. Since for this particluar problem the influence of flux boundary condition on the cavity surface acts as a sphere centered at the origin, only four
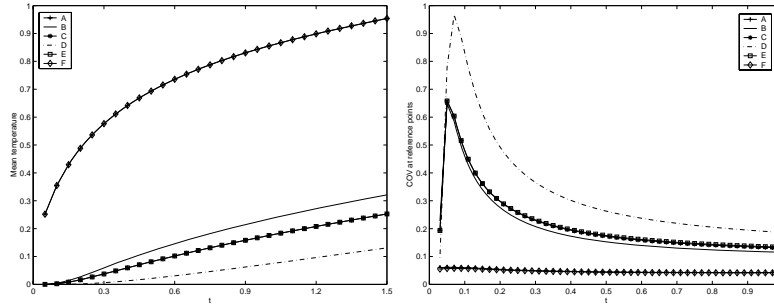
reference points are considered.

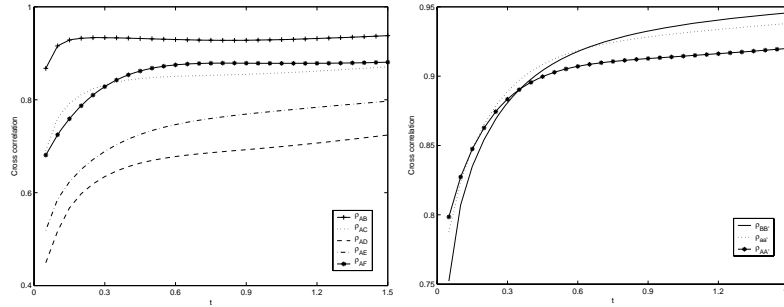Figure 4: Temperature evolution at reference points on $y = 0$. Left: mean temperature. Right: COV.

Figure 5: Cross-correlation coefficients on reference points. Left: with respect to point A on $y = 0$. Right: between $y = 0$ and $y = 1$ along the vertical centerline.

6 Summary

A three-dimensional parallel stochastic spectral method based on generalized polynomial chaos is developed for steady and unsteady heat conduction problems. The algorithm takes advantage of parallel computing to deal with the large system with about *150 million unknowns* resulted from a relatively small correlation length in the Karhunen-Loeve decomposition. For the steady case, polynomial chaos is more than 10 (10,000/780) times faster than Monte Carlo simulations. For the unsteady case, the expected speed-up is even more as was indicated in two-dimensional simulations in [25]. The efficiency of polynomial chaos depends greatly on the dimensionality of the random space. The size of the system of equations that needs to be solved grows rapidly as the number of stochastic dimensions and polynomial order increases. We will address this
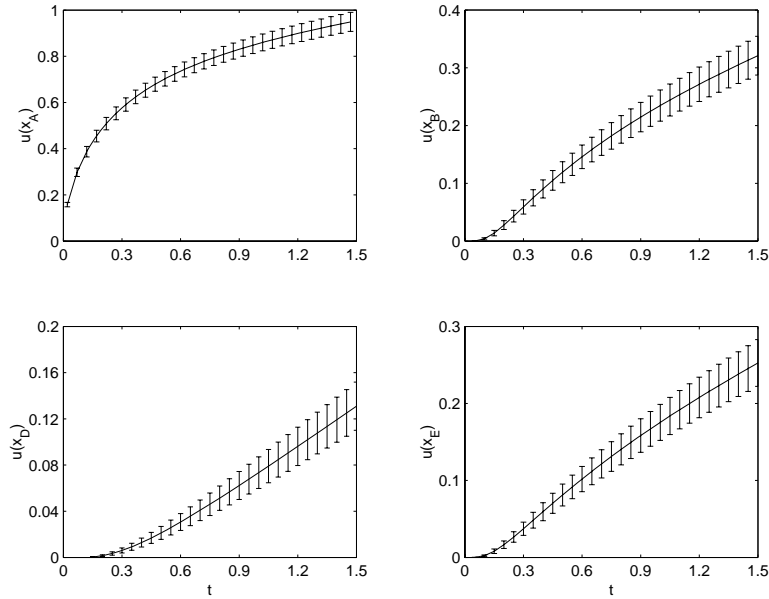
8

Figure 6: Temperature evolution at reference points on $y = 0$.

References

[1] N. Wiener. The homogeneous chaos. *Amer. J. Math.*, 60:897–936, 1938.

[2] M. Kleiber and T. D. Hien. *The stochastic finite element method.* John Wiley & Sons Ltd, 1992.

[3] W. K. Liu, T. Belytschko, and A. Mani. Probabilistic finite elements for nonlinear structural dynamics. *Comput. Methods Appl. Mech. Engrg.*, 56:61–81, 1986.

[4] W. K. Liu, T. Belytschko, and A. Mani. Random field finite elements. *Int. J. Num. Meth. Engng.*, 23(10):1831–1845, 1986.

[5] E. H. Vanmarcke and M. Grigoriu. Stochastic finite element analysis of simple beams. *J. Eng. Mech*, 109(5):1203–1214, 1983.

[6] M. Shinozuka and G. Deodatis. Response variability of stochastic finite element systems. *J. Eng. Mech.*, 114(3):499–519, 1988.

[7] F. Yamazaki, M. Shinozuka, and G. Dasgupta. Neumann expansion for stochastic finite element analysis. *J. Eng. Mech.*, 114(8):1335–1354, 1988.

[8] W. Q. Zhu, Y. J. Ren, and W. Q. Wu. Stochastic FEM based on local average of random vector fields. *J. Eng. Mech.*, 118(3):496–511, 1992.

[9] G. Deodatis. Weighted integral method. I: stochastic stiffness matrix. *J. Eng. Mech.*, 117(8):1851–1864, 1991.

[10] G. Deodatis and M. Shinozuka. Weighted integral method. II: response variability and reliability. *J. Eng. Mech.*, 117(8):1865–1877, 1991.

[11] R. G. Ghanem and P. Spanos. *Stochastic Finite Eelements: A Spectral Approach.* Springer-Verlag, New York, 1991.

[12] R. G. Ghanem. Stochastic finite elements for heterogeneous media with multiple random non-gaussian properties. *ASCE J. Engrg. Mech.*, 125(1):26–40, 1999.

[13] R. G. Ghanem and J. Red-Horse. Propagation of uncertainty in complex physical systems using a stochastic finite elements approach. *Physica D*, 133:137–144, 1999.

[14] R. G. Ghanem. Ingredients for a general purpose stochastic finite element formulation. *Comput. Methods Appl. Mech. Engrg.*, 168:19–34, 1999.

[15] D. Xiu and G. E. Karniadarkis. The Wiener-Askey polynomial chaos for stochastic differential equations. *SIAM J. Sci. Comput.*, 24(2):619–644, 2002.

[16] D. Xiu and G. E. Karniadarkis. Modeling uncertainty in steady state diffusion problems via generalized polynomial chaos. *Comput. Methods Appl. Math. Eng.*, 191:4927–4948, 2002.

[17] D. Xiu and G.E. Karniadakis. Modeling uncertainty in flow simulations via generalized polynomial chaos. *J. Comput. Phys.*, 187:137–167, 2003.

[18] I. Babuška and P. Chatzipantelidis. On solving elliptic stochastic partial differential equations. *Comput. Methods Appl. Mech. Engrg.*, 191:4093–4122, 2002.

[19] I. Babuška, R. Tempone, and G. E. Zouraris. Galerkin finite element approximations of stochastic elliptic differential equations. Technical Report 02-38, TICAM, 2002.

[20] M. K. Deb, I. Babuška, and J. T. Oden. Solution of stochastic partial differential equations using Galerkin finite element techniques. *Comput. Methods Appl. Mech. Engrg.*, 190:6359–6372, 2001.

[21] M. Loeve. *Probability Theory, fourth ed.* Springer-Verlag, New York, 1977.

[22] G. E. Karniadakis and S. J. Shervin. *Spectral/hp element methods for CFD.* Oxford University Press, 1999.

[23] K. E. Atkinson. *The Numerical Solution of Integral Equations of the second kind.* Cambridge University Press, 1997.

[24] R. B. Lehoucq and D. C. Sorensen. Deflation techniques for an implicitly restarted arnoldi iteration. *SIAM Matrix Analysis and Applications*, 17(4):789–821, 1996.

[25] D. Xiu and G. E. Karniadarkis. A new stochastic approach to transient heat conduction modeling with uncertainty. *Int. J. Heat Mass Trans.*, 46(24):4681–4693, 2003.